

Sbor. geol. věd	Užitá geofyz., 24	Pages 71–89	11 figs.	1 tab.	— pl.	Praha 1990 ISSN 0036-5319
--------------------	----------------------	----------------	-------------	-----------	----------	------------------------------

## Presentation of results of the IP field measurements in maps and sections

## Представление результатов полевых измерений ВП на картах и разрезах

Miloš Karous<sup>1</sup>

Received June 12, 1987

*Induced polarization  
Pseudosections  
Electrical methods  
Polarizability*

Karous, M. (1990): Presentation of results of the IP field measurements in maps and sections. — Sbor. geol. Věd, užitá Geofyz., 24, 71–89. Praha.

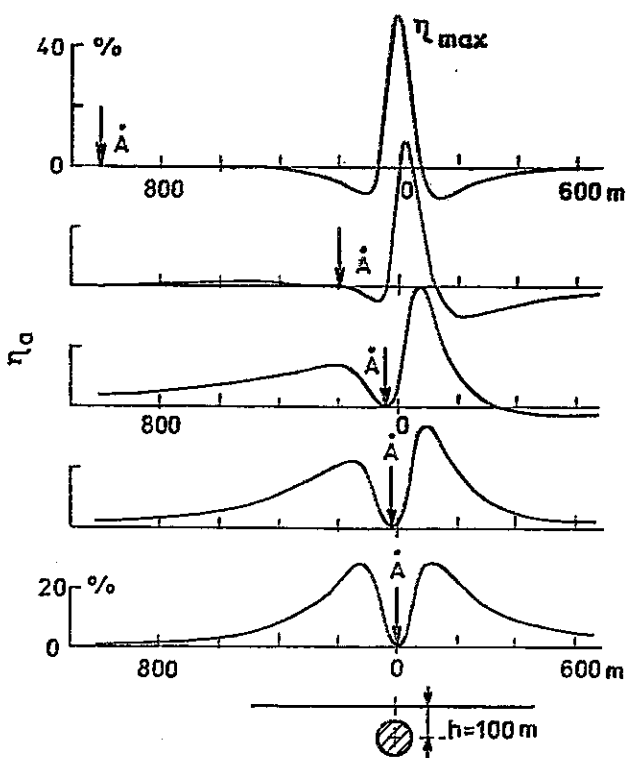
Abstract: New ways of processing of area and profile measurements by the IP method in the time and frequency domains by means of modified values of apparent polarizability are suggested. The configuration of modified polarizability anomalies in maps and sections better corresponds to the actual distribution of anomalous polarizability, thus making it possible to obtain a more reliable geoelectric model of the investigated region. In a similar manner it is possible to process also simultaneous resistivity measurements. The interpretation of both resistivity and polarizability data arranged into the suggested schemes is less ambiguous, simpler and more illustrative than that based on resistivity and polarizability pseudoschemes constructed in "classical" ways as pseudosections.

<sup>1</sup> *Katedra užitě geofyziky přírodovědecké fakulty Univerzity Karlovy, Albertov 6, 128 43 Praha 2*

### Introduction

This paper is dedicated to the possibility of determining the position and extension of anomalously polarized geological bodies. This problem is the one most frequently solved by the IP method. However, unambiguous procedures have not yet been developed for interpretations of buried anomalous bodies. In majority of cases we have been satisfied with the qualitative interpretation when on the basis of our experience in interpreting and using a limited set of theoretical model curves some geometrical parameters (shape and position of anomalous body)

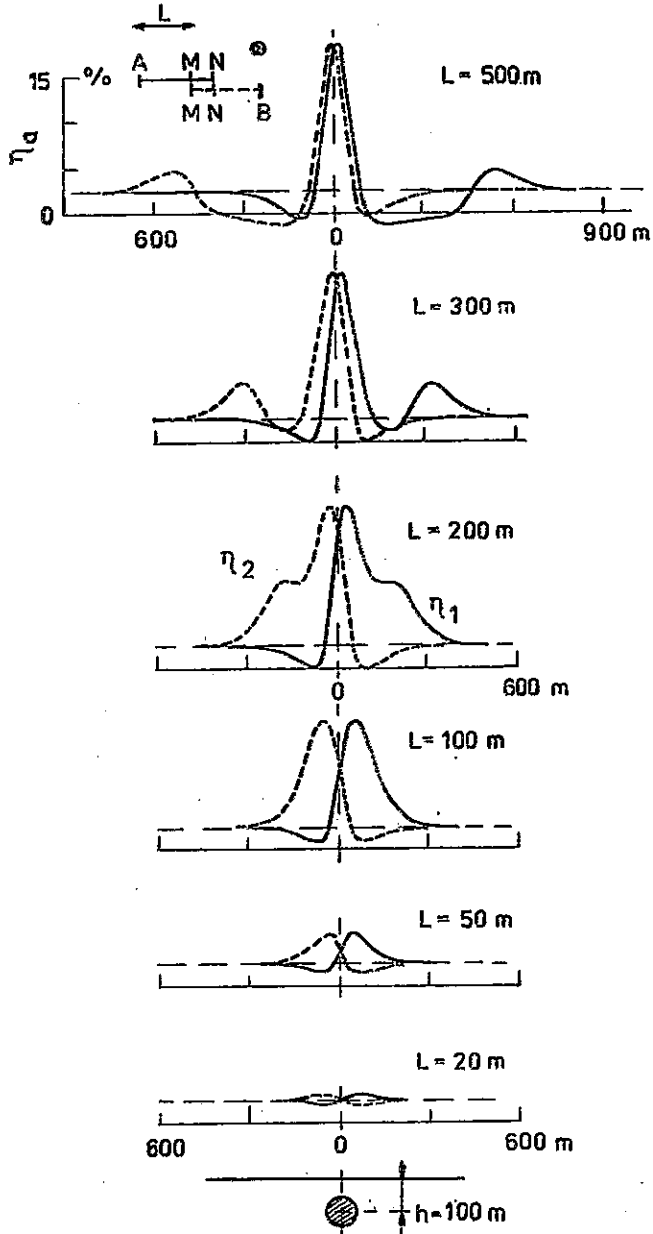
have been estimated directly from a particular graphical presentation of apparent polarizability data or other parameters derived from the IP measurements. As it will be shown in the paper, the classical graphical presentation of the measured parameters has not always been suitable, for the extremes (maxima) of the apparent polarizability do not appear directly above the anomalous object. The shift of the maximum depends on the electrode configuration used, on the shape, dimensions and depth of the anomalous object as well as on other factors. An anomalous object is frequently manifested by numerous local extremes which could be misinterpreted as caused by other objects. The possibilities of constructing more illustrative schemes – maps and vertical sections – will be shown, which better correspond to the actual distribution of polarizability than the “classical” ones, so that dimensions and the space distribution of investigated anomalously polarized bodies can be directly interpreted from them. The ways suggested in this article for processing the data obtained by the IP method can analogically be used also for processing the resistivity measurements taken simultaneously with the IP measurements.



1. Apparent polarizability curves above a polarizable sphere for the three-electrode gradient configuration AMN with fixed current electrode  $A$  for various positions of grounding

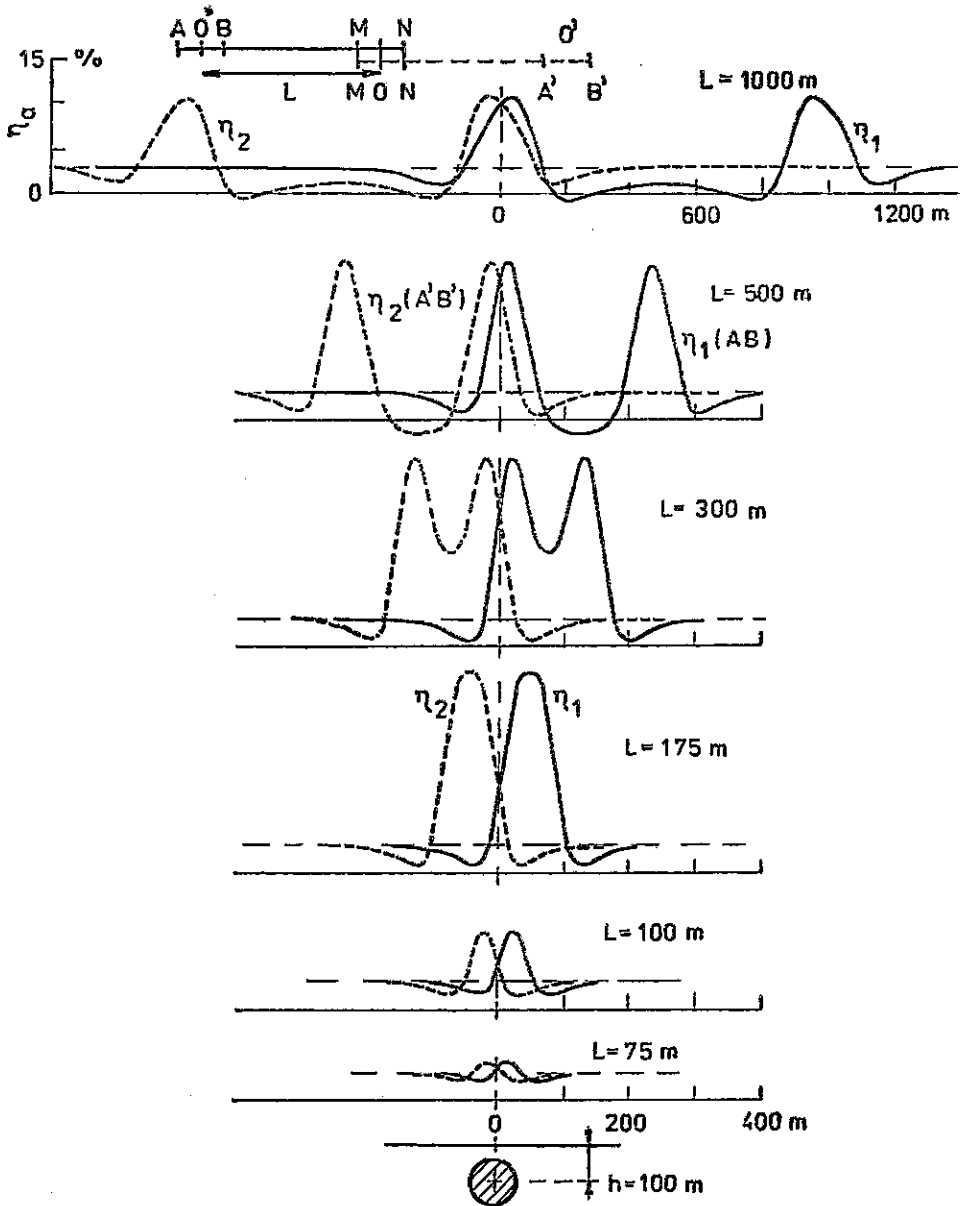
## Profile curves and polarizability maps

Maps of isolines of measured or simply transformed data represent, to various (mostly small) extent, the actual distribution of polarizability. They have usually been constructed from values obtained from measurements along parallel profiles the distance of which is defined by the scale of a particular survey to cover the

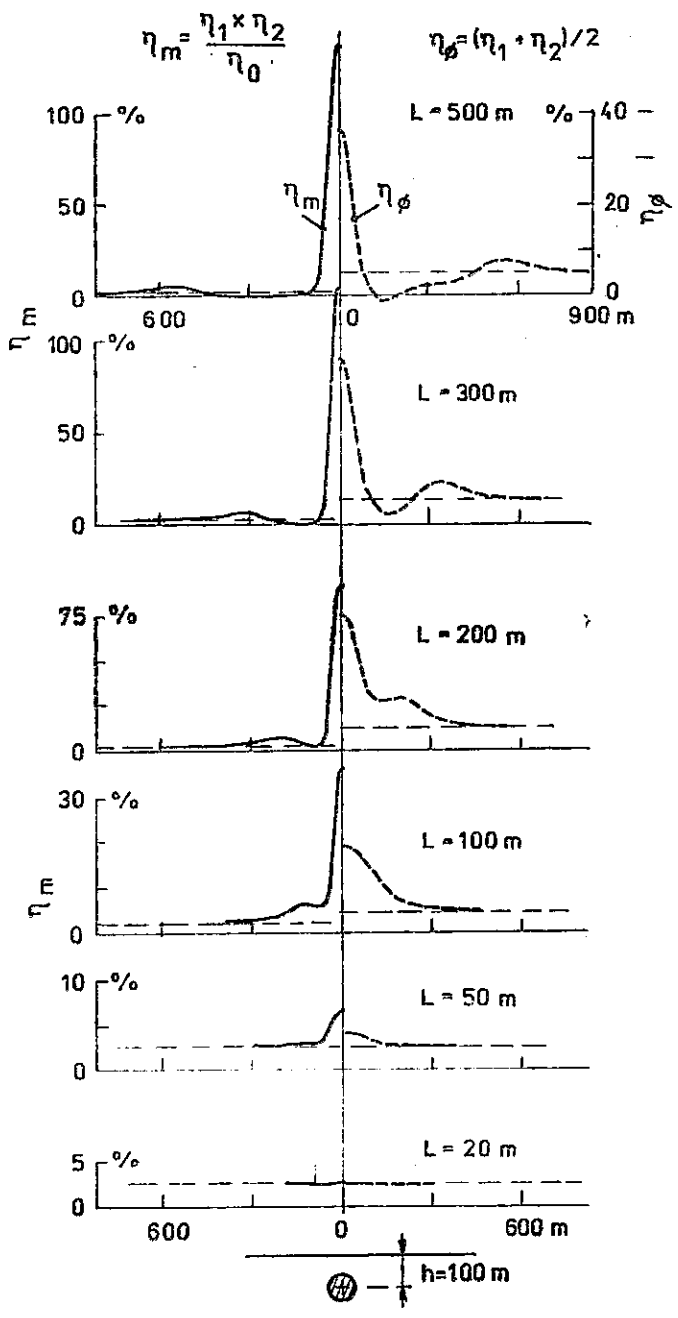


2. Apparent polarizability curves above a polarizable sphere for the combined profiling of various lengths  $L = AB/2$

study area. Using different electrode configuration above the same anomalous object, different profile curves are obtained. Above one object, profile curves exhibit, in majority of cases, several extremes corresponding to the passage of individual electrodes or dipoles over the object at depth.

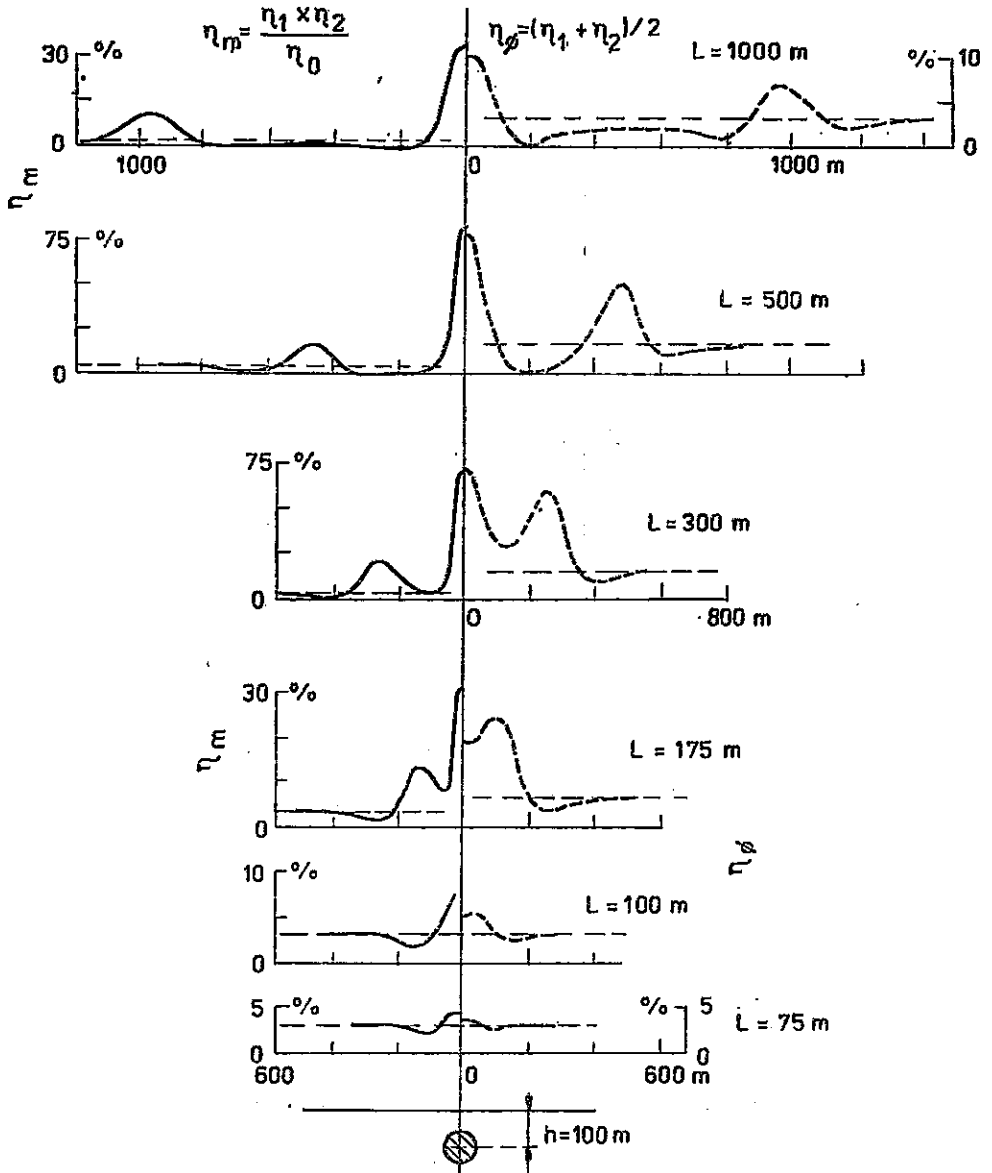


3. Apparent polarizability curves above a polarizable sphere for the dipole-dipole profiling of various lengths  $L = OO'$



4. Modified polarizability  $\eta_m$  and mean polarizability  $\eta_\phi$  curves above a polarizable sphere for the combined profiling

In order to map polarized bodies it is more suitable to use an electrode configuration with fixed grounding of current electrodes for which extremes are to be formed only when the moved potential dipole passes over an anomalous body. Among these configurations the most frequently applied is the one called the gradient



5. Modified polarizability  $\eta_m$  and mean polarizability  $\eta_\phi$  curves above a polarizable sphere for the dipole-dipole profiling

array (GA) and/or the so called combined gradient array (CGA) represented by two pole-dipole arrays in which the third current electrode is situated at a relatively long distance. Considering the justification of using particular arrays to explore anomalous objects and taking into account the depth of their investigation it is most suitable to analyze the profile curves above a locally limited object, preferably of an isometric form (e.g. a sphere). Using the GA modification apparent polarizability curves  $\eta_a$  exhibit maximum directly above the object of increased polarizability, similarly as in the CGA modification for the current electrode  $A$  grounded at a relatively long distance from the object (upper part of Figure 1). The anomalous object being close to one of the groundings in the GA modification the maximum is shifted similarly as in the CGA modification because the influence of the second grounding is negligible (Figure 1). If the grounding is very close to the epicentre of the object or even directly above the object, two maxima of apparent polarizability appear on both sides of the grounding (lower part of Figure 1). The magnitude of the shift of the extreme is proportional to the depth of the object  $h$ .

In the case of symmetrical configuration with moving current electrodes (i.e. the Schlumberger and Wenner profilings) the anomalous curve above the sphere shows three maxima. The central (the largest) one corresponds to the position of the polarized sphere. Asymmetric electrode configurations (i.e. dipole-dipole and combined two pole-dipole arrays) yield two curves of apparent polarizability  $\eta_1$  and  $\eta_2$ , each of them exhibiting two maxima (figures 2 and 3). In the case of objects at greater depths both maxima can merge into a broader one. Then, in such a case, there is a problem to construct maps of isolines. It is usual to plot the mean values of polarizability  $\eta_\sigma$  (figures 4 and 5 – broken line):

$$\eta_\sigma = \frac{1}{2}(\eta_1 + \eta_2). \quad (1)$$

Particularly in the case of dipole-dipole profiling the curves of mean polarizability  $\eta_\sigma$  exhibit expressive false maxima on both sides of the object at distances that equal the length  $L$ , i.e. the electrode separation. In the map of isolines, the number and positions of anomalous objects can be incorrectly interpreted.

In the case of asymmetric electrode configuration out of the two maxima of both curves, however, only one is located above the object. It is therefore suitable to substitute the mean values of polarizability with the simplest correlation, i.e. with the product of values of both polarizabilities divided by normal value of polarizability  $\eta_0$  typical of the nonanomalous parts of the region investigated. Let the value obtained in this way be called a modified polarizability  $\eta_m$ :

$$\eta_m = \frac{\eta_1 \times \eta_2}{\eta_0}. \quad (2)$$

Curves of modified polarizability do not show such expressive false maxima away from the anomalous object (figures 4 and 5 – left-hand part, solid line).

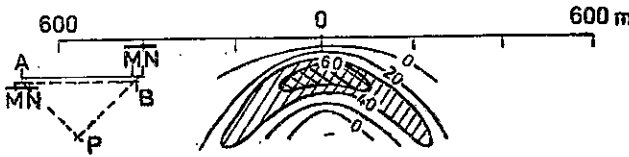
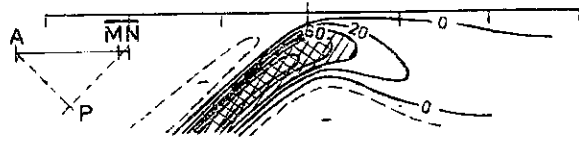
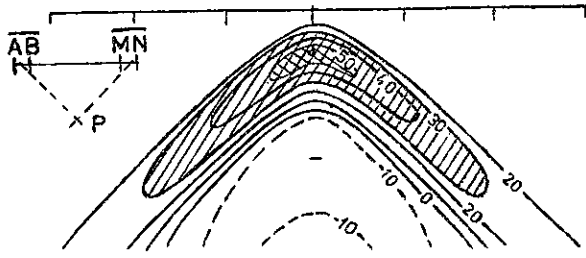
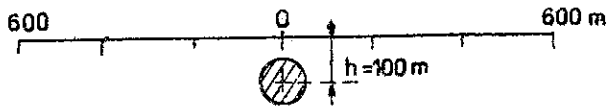
## Vertical sections of polarizability

It has been said that for the mapping of polarizable objects the GA modification is most suitable as the maximum of the curve is located directly above the object. A disadvantage of the GA is in its low ability to differentiate the sources of anomaly at depth. For more detailed investigations of depth relations of polarizable objects it is necessary to apply an electrode configuration with controlled extent of the depth of investigation, e.g. by a change of length  $L$  of the electrode configuration (for the Schlumberger and combined profilings  $L = AB/2$ , in the case of the dipole-dipole profiling  $L$  is the distance  $OO'$  between the centres of the potential and current dipoles). In the case of these configurations vertical pseudosections of the apparent polarizability have been constructed, so that the measured values of apparent polarizability have been plotted at points  $P$  in the vertical section beneath the investigated profile. Positions of points  $P$  are given by the centre of the electrode configuration used and the length  $L/2$  (Figure 6). The values at points  $P$  have then been interpolated. In this way a map of isolines of apparent polarizability has been obtained. Thus the construction has been quite simple. The value of this construction is, despite its simplicity, considerably reduced because the courses of isolines in the section do not correspond to the shape of the anomalous body (Figure 6). For example, above the studied objects of isometric form false "shadows" occur in the section, extending downward from the position of the object under the angle of  $45^\circ$ . At the crossing of two false "shadows" due to two different objects an intensive unreal anomaly develops which could be erroneously interpreted as caused by another object. "Classical" pseudosections can thus be interpreted correctly only with the use of a large set of model pseudosections.

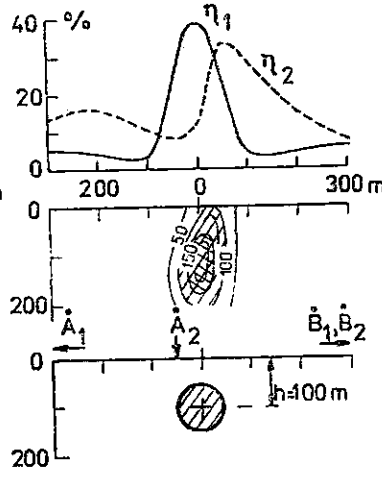
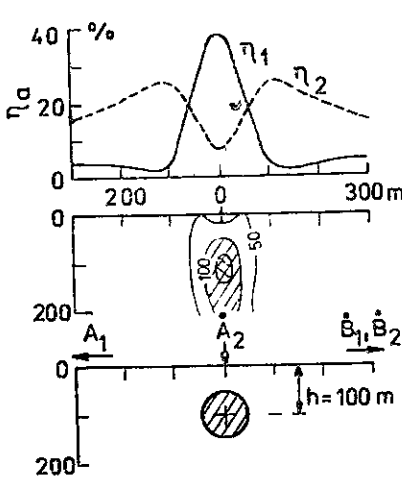
By using the different shifts of two curves of asymmetric electrode configuration measurements it is possible to construct vertical pseudosections from the IP profiling with only one electrode spacing. It is necessary, however, to carry out bilateral measurements by two asymmetric configurations, i.e. measurements at the position of current pole or dipole on both sides of the measuring dipole. It has been discovered (Komarov 1980) that in the CGA modification the maxima of apparent polarizability are located at points  $M$  which are equally distant from the current grounding  $A$  as is the centre  $S$  of the polarizable sphere from the grounding  $A$ , i.e.  $AM = AS$ . This has also been proved theoretically (Karous 1983). In order to determine the position of the sphere and its depth two measurements should be performed for two different positions of current groundings  $A_1$  and  $A_2$ . The centre of the sphere is directly at the intersection of two arcs plotted through points  $M_1$  and  $M_2$  corresponding with the maxima of polarizability  $\eta_{1 \max}$  and  $\eta_{2 \max}$ , with centres at groundings  $A_1$  and  $A_2$ .

The interpretation method of Komarov has been generalized and extended for





6. "Classical" pseudosections of apparent polarizabilities above a polarizable sphere for the dipole-dipole profiling with several lengths of separation of electrode configuration  $ABMN$  for the three-electrode configuration  $AMN$ , and for the combined profiling  $AMN, MNB$



7. Vertical modified pseudosections constructed from the model curves of polarizability above a polarizable sphere for the asymmetric configuration  $AMN$  with fixed current grounding  $A$  in two different positions  $A_1$  and  $A_2$

construction of vertical pseudosections from two measurements with fixed current groundings (Karous 1983, 1985). The method of construction is very simple. To each intersection  $P_{ij}$  of two arcs with centres at  $A_1$  and  $A_2$  which pass through the points of measurements  $x_i$  and  $x_j$ , the value of modified polarizability can be assessed according to the expression:

$$\eta_m(P_{ij}) = \frac{\eta_1(x_i) \times \eta_2(x_j)}{\eta_0}, \quad (3)$$

which can then be used for construction of isolines. In this way the so called modified pseudosection will be obtained. It is obvious that the modified polarizability reaches its maximum if the point  $P_{ij}$  lies at the intersection of arcs passing through the maxima  $\eta_{1 \max}$  and  $\eta_{2 \max}$ . Thus the extreme values of  $\eta_m$  in the section correspond to the position of polarizable objects.

Examples of sections constructed in this way from the model curves above the polarizable sphere are shown in Figure 7. Contrary to "classical" pseudosections the modified pseudosections exhibit extreme values without false "shadows" and in the position of the anomalous object only. As it has been verified for models of other shapes (i.e. sheetlike, ellipsoidal etc.), also in these cases the form of isolines in modified sections corresponds to the shape of the polarizable object.

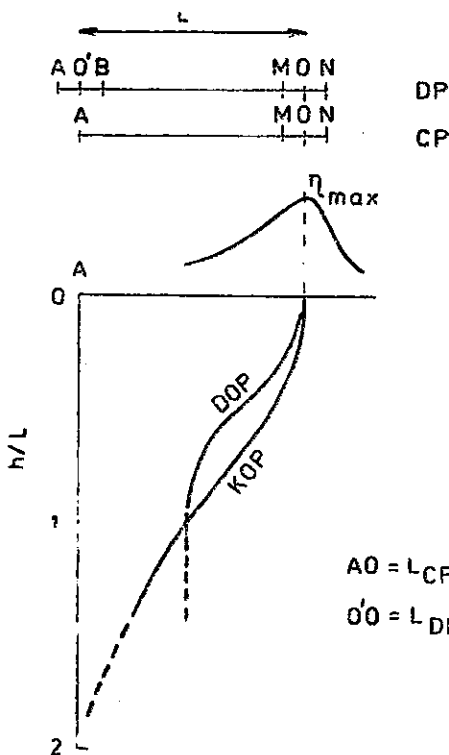
Analogically, vertical pseudosections can be constructed also from measurements taken using asymmetric configurations with current electrodes moving in one spacing only. From the model and theoretical curves obtained above the sphere using dipole-dipole and combined profilings, the relation has been studied between the centre of isometric body position and the position of maximum of measured apparent polarizabilities. Beneath the maximum the position of the centre can lie on the curve (the so called depth curve) which is plotted in Figure 8 for the combined (CP) and dipole-dipole (DP) profilings. The search for a sphere to depths smaller than the length of separation  $L$  is justified only because spheres at greater depths manifest themselves by very weak anomalies. The position of an isometric object at the intersection of two depth curves corresponds to both positions of the current pole or dipole.

Two depth curves can be drawn through each point of measurements (corresponding to the left and right current source). These depth curves form a network of intersecting points  $P_{ij}$  to which values of the modified polarizability are positioned according to relation (3). By interpolating the resulting isolines the modified pseudosections are obtained for the combined or dipole-dipole profilings. Examples of such pseudosections for the polarized sphere are shown in figures 9 and 10. Positions of points  $P_{ij}$  need not be determined graphically. In order to enable the automatic data processing it is advantageous to make tables of coordinates  $x_{ij}$  and  $h_{ij}$  of points  $P_{ij}$  in the section. For the coordinates the following relation

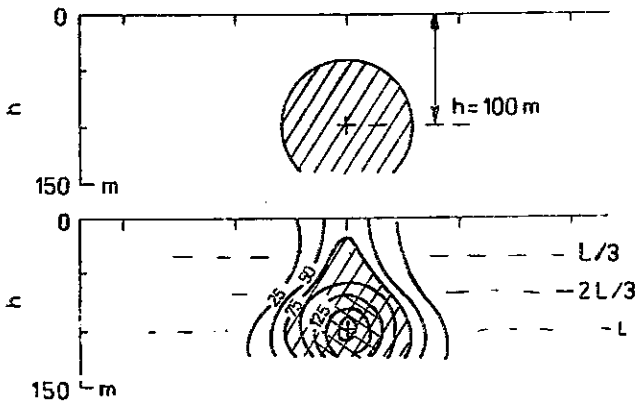
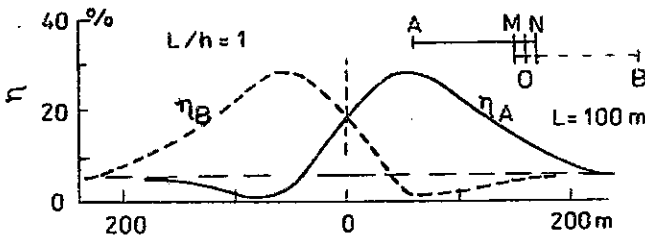
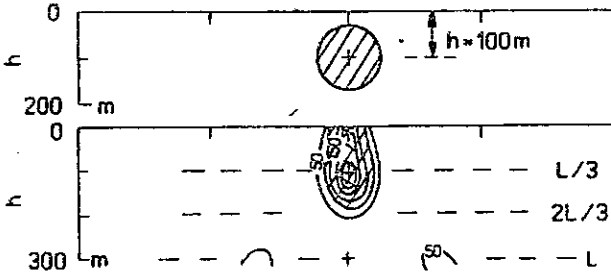
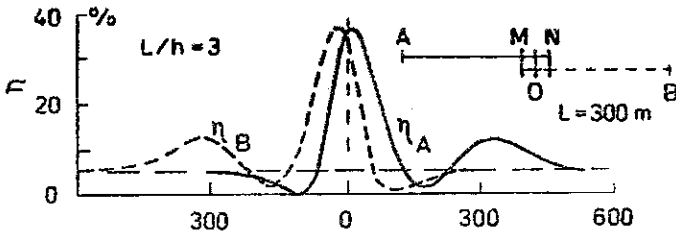
Table 1

Depth coefficients  $\alpha_n^m$  for constructing vertical modified pseudosection from combined and dipole-dipole profilings

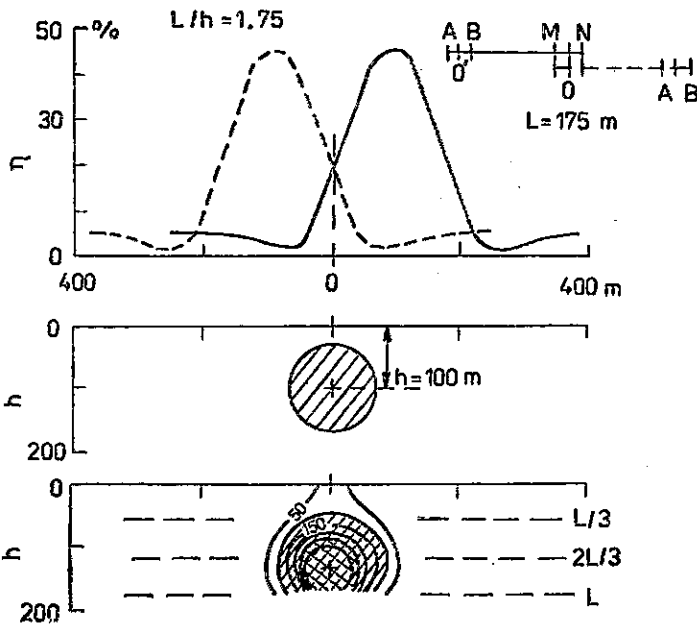
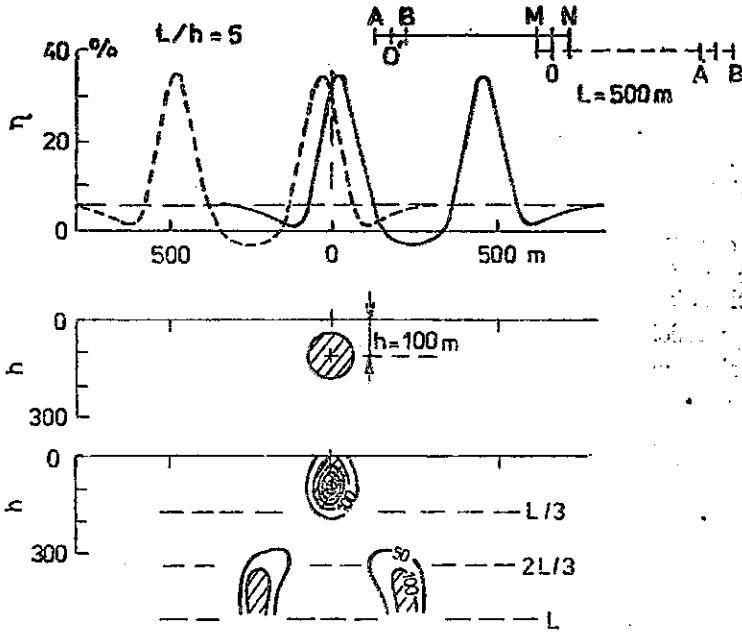
Combined profiling						Dipole profiling					
m	n					m	n				
	3	4	5	6	7		3	4	5	6	7
0	0.00	0.00	0.00	0.00	0.00	0	0.00	0.00	0.00	0.00	0.00
1	0.54	0.47	0.42	0.39	0.36	1	0.38	0.32	0.28	0.25	0.23
2	0.77	0.66	0.60	0.54	0.50	2	0.54	0.46	0.42	0.38	0.34
3	0.99	0.82	0.73	0.66	0.62	3	0.92	0.58	0.59	0.46	0.42
4	1.24	0.99	0.85	0.77	0.72	4		0.91	0.62	0.54	0.49
5		1.18	0.99	0.88	0.80	5			0.91	0.66	0.56
6		1.42	1.15	0.99	0.89	6				0.92	0.68
7			1.34	1.11	0.99	7					0.91
8				1.24	1.10						
9				1.43	1.22						
10					1.35						



8. Depth curves for a polarizable sphere (i.e. the curves on which the centre of sphere is located for the given position of the apparent polarizability maximum) for the dipole-dipole (DP) and combined (CP) profilings



9. Modified vertical pseudosections of polarizability derived from the combined profiling measurements with two different separations above a polarizable sphere



10. Modified vertical pseudosections of polarizability derived from the dipole-dipole profiling above a polarizable sphere for various lengths of electrode separations  $L = 00'$

is valid:

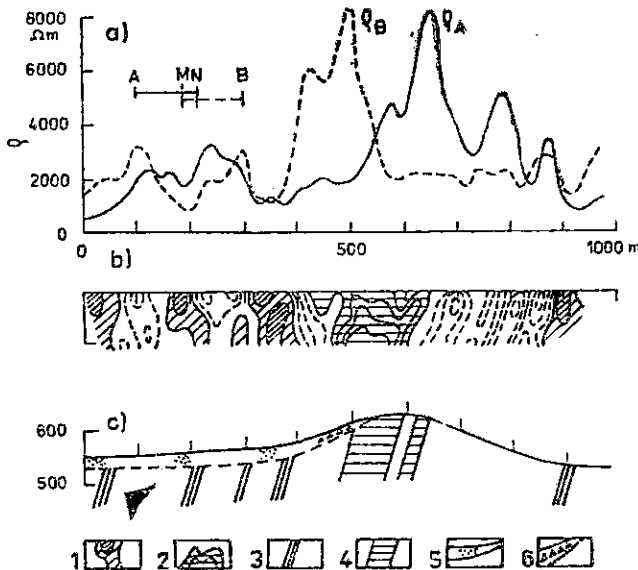
$$x_{ij} = \frac{1}{2}(x_i + x_j) = \frac{i+j}{2} \Delta x, \quad (4)$$

$$h_{ij} = h_m = L \cdot \alpha_{|i-j|}^n = L \cdot \alpha_m^n, \quad (5)$$

where  $n = L/\Delta x$  is the ratio of the length of separation  $L$  to the measurement interval  $\Delta x$ ,  $x_i = i \cdot \Delta x$  and  $x_j = j \cdot \Delta x$  are points of measurements,  $m = |i - j|$  is the relative distance of points of measurements. It is equal to  $m = |x_i - x_j|/\Delta x$ . The depth coefficients  $\alpha_m^n$  derived from the depth curves for isometric inhomogeneities for various  $m$  and  $n$  are presented in Table 1. Despite the fact that in Table 1 the depth coefficients  $\alpha_m^n$  are larger than 1.0, it is justified to construct the sections only to depths smaller than the length  $L$ .

11. An example of the modified vertical resistivity pseudosection derived from the field measurements using the combined profiling method at the locality Rejvíz in the Jeseníky Mts.

*a* - resistivity profiling curves, *b* - vertical modified resistivity pseudosection, *c* - interpreted geological section; 1 - conductors in the isoohm section, 2 - nonconductors in the isoohm section, 3 - interpreted conductive zones (graphitized rocks), 4 - interpreted non-conductive zones (quartzite rocks), 5 - solid products of weathering of graphitized rocks in the eluvium, 6 - screes of quartzite rocks



The verification of the vertical modified pseudosections obtained above models of bodies of other shapes, including irregular ones, proves a relatively higher effectiveness of the suggested construction method. In a similar manner the resistivity data can also be displayed. An example of a resistivity section and the resulting interpretation of resistivity measurements obtained by the combined profiling is shown in Figure 11.

*K tisku doporučil J. Hanzlík*

*Přeložil autor*

### References

- Baudoin, B. (1968): Etude au laboratoire de la methode de polarisation provoquee. — Bull. BRGM, Sect. Orléans.
- Bertin, J.—Loeb, J. (1976): Experimental and theoretical aspects of induced polarization. — Geoexploration Monographs, 1, 7, Gebrüder Borntraeger. Stuttgart—Berlin.
- Cole, K. S.—Cole, R. H. (1941): Dispersion and absorption in dielectrics. — J. Chem. Phys., 9, 341—351. London.
- Collet, L. S. (1959): Laboratory investigation of overvoltage. In J. R. Wait: Overvoltage research and geophysical application. — Pergamon Press. New York.
- Csorgei, J. et al. (1983): Time domain IP equipment and method for source discrimination. — Geophys. Transactions, 29, 4, 21—32. Budapest.
- DeWitt, G. W. (1978): Parametric studies of induced polarization spectra. — M. Sc. thesis, Univ. of Utah. Salt Lake City.
- Erkel, A. et al. (1979): Measurements and interpretation of the dynamic characteristics of induced polarization decay curves. — Geophys. Transactions, 25, 65—81. Budapest.
- Gennadinik, B. I.—Melnikov, V. P.—Gennadinik, G. B. (1976): Teorija vyzvannoj élektrochimickéskoj aktivnosti gornych porod. — Jakutskoe knižnoe izdatel'stvo. Jakutsk.
- Grissemann, C. (1971): Examination of the frequency-dependent conductivity of ore-containing rock on artificial models. — Sci. Rep. 2, Electr. Lab. Univ. of Innsbruck. Innsbruck.
- Hallof, P. G. et al. (1979): The use of the Phoenix IPV-2 phase IP receiver for discrimination between sulphides and graphite. — Paper presented at the SEG Ann. Meeting in New Orleans. Tulsa.
- Joffe, L. M. et al. (1979): Metodika raboty s geoélektričeskoy apparaturoj SVP-74. — Naučno-proizvodnoe ob'edinenie Geofizika. Leningrad.
- Kanasewich, E. R. (1975): Time sequence analysis in geophysics. — The Univ. Alberta Press. Alberta.
- Karous, M. (1983): Induced polarization anomaly above a sphere. — Geoexploration, 21, 49—63. Amsterdam.
- (1985): Zpracování geoelektrických měření v geologickém mapování v rudní prospekci a hydrogeologickém a inženýrskogeologickém průzkumu. — D. Sc. thesis, Charles Univ. Praha.
- Kněž, J. (1985): Určení dynamických parametrů vyzvané polarizace. — Sbor. prací 8. celost. konf. geof. Č. Budějovice.
- Komarov, V. A. (1965): Vremennye charakteristiki vyzvannoj poljarizacii. — Metod. Techn. Razv., 49, 29—62. Leningrad.
- (1980): Élektrozazvedka metodom vyzvannoj poljarizacii. — Nedra. Leningrad.
- Komarov, V. A.—Šubnikova, K. G. (1976): O svjazi vremennyh parametrov vyzvannoj poljarizacii s razmerom poljarizuemych tel. — Met. Razvit. Geofiz., 26, 103—114. Leningrad.

- Lee, T. (1981): Short note on the Cole-Cole model in time-domain induced polarization. — *Geophysics*, 46, 932–938. Tulsa.
- Lemec, V. I. et al. (1973): K metodike rabot po metodu INFAZ-VP s ustanovkoj gradienta. — *Vopr. rud. Geofiz.*, 5, 42–48. Alma-Ata.
- Ljachov, L. L.–Melnikov, V. P. (1968): O vozmožnostjach ispolzovanija fazovočastotnyh charakteristik VP dlja klassifikacii anomalij poljarizuemosti. — *Izd. Vuzov, Ser. Geof. Razv.*, 7, 153–154. Moskva.
- Major, J.–Silic, J. (1981): Restrictions on the use of Cole-Cole dispersion models in complex resistivity interpretation. — *Geophysics*, 46, 6, 916–931. Tulsa.
- Olhoeft, G. R. (1982): Electrical properties of rocks and minerals. — University course notes. Golden.
- Pelton, W. H. (1977): Interpretation of induced polarization and resistivity data. — Ph. D. thesis, Univ. of Utah, Salt Lake City.
- Pelton, W. H. et al. (1978a): Inversion of two-dimensional resistivity and induced polarization data. — *Geophysics*, 43, 4, 788–803. Tulsa.
- (1978b): Mineral discrimination and removal of inductive coupling with multifrequency IP. — *Geophysics*, 43, 3, 588–609. Tulsa.
- (1983): Interpretation of complex resistivity and dielectric data, Part I. — *Geophys. Transactions*, 29, 4, 94–99. Budapest.
- Verö, L. et al. (1985): Comparison of interpretation methods for time domain spectral induced polarization data. — *Geophys. Transactions*, 31, 1–3, 182–188. Budapest.
- Wait, J. R. (1984): Relaxation phenomena and induced polarization. — *Geoexploration*, 22, 345–355. Amsterdam.
- Wong, J. (1979): An electrochemical model of the induced polarization phenomenon in disseminated sulfide ores. — *Geophysics*, 44, 7, 1245–1265. Tulsa.



## Представление результатов полевых измерений ВП на картах и разрезах

(Резюме английского текста)

Miloš Karous

Представлено 12-го июля 1987 г.

В этой статье предложен новый способ презентации результатов полевых измерений величины вызванной поляризации (ВП) в виде т. наз. модифицированных карт изолиний и вертикальных разрезов, позволяющих быстро и объективно интерпретировать положение, форму и размеры аномально поляризуемых геологических объектов в виде горизонтальной плоскости и вертикальном разрезе под измеряемым профилем. Современное состояние разработки автоматической интерпретации на вычислительных машинах пока не позволяет эффективно использовать обработку данных профилей на ЭВМ в обыкновенных рабочих условиях геофизических исследований, поэтому предложенный способ может пополнить пробел в интерпретационных приемах метода вызванной поляризации.

До сих пор результаты метода ВП представляются в виде кривых кажущейся поляризуемости (рис. 1–3). Максимумы кривых кажущейся поляризуемости, однако, часто не совпадают с расположением аномально поляризуемых тел, в связи с чем карты изолиний не могут дать полное представление о расположении аномальных зон. Поэтому были введены т. наз. модифицированные данные поляризуемости (формулы 2 и 3), кривые которых имеют экстремумы над поляризуемыми телами (рис. 4 и 5).

Результаты профилирования методом ВП, использующего несколько различных расстановок питающих электродов, изображаются часто в виде „классических“ псевдоразрезов, но характер изолиний в них не отвечает истинной форме аномального тела (рис. 6). Поэтому в этой статье предлагается строить модифицированные разрезы с использованием модифицированных данных поляризуемости. Эти данные вписываются в разрезах в точки пересечения кривых, в которых на различных глубинах лежат сферы со совпадающими максимумами кажущейся поляризуемости (рис. 8). Форма изолиний в модифицированных разрезах отвечает приблизительно форме вертикального разреза аномально поляризуемого геологического тела (рис. 7, 9 и 10).

Сходно с тем строятся вертикальные модифицированные разрезы по данным модифицированных сопротивлений, измеряемых при применении метода ВП вместе с кажущимися поляризуемостями (рис. 11).

*Přeložil autor*